Spatio-temporal constraints for emissivity and surface temperature retrieval: preliminary results and comparisons for SEVIRI and IASI observation

Marilena Amoroso[1], Italia De Feis[2], Guido Masiello[1], Carmine Serio[1], Sara Venafra[1] and Philip Watts[3]

[1] *University of Basilicata, School of Engineering, Potenza, Italy; marilena.amoroso@libero.it, guido.masiello@unibas.it, carmine.serio@unibas.it, sara.venafra@unibas.it*
[2] *Istituto per le Applicazioni del Calcolo "M. Picone" (CNR), Napoli, Italy; i.defeis@iac.cnr.it*
[3] *EUMETSAT, Darmstadt, Germany; Philip.Watts@eumetsat.int*

Abstract. Infrared instrumentation on geostationary satellites is now rapidly approaching the spectral quality and accuracy of modern sensors flying on polar platforms. Currently at the core of EUMETSAT geostationary meteorological programme is the Meteosat Second Generation (MSG). However EUMETSAT is preparing for Meteosat Third Generation (MTG). The capability of geostationary satellites to resolve the diurnal cycle and hence to provide time resolved sequences or times series of observations is a source of information which could suitably constrain the derivation of geophysical parameters. Nowadays, also because of lack of time continuity, when dealing with observations from polar platforms, the problem of deriving geophysical parameters is normally solved by considering each single observation as independent from past and future events. For historical reason, the same approach is currently pursued with geostationary observations, which are still now dealt with as they were polar observations. In this presentation we show some preliminary results on emissivity and surface temperature retrieval for SEVIRI observations, using the Kalman filter methodology and the times accumulation approach and compare the retrievals with those obtained using IASI observations co-localized with SEVIRI ones. We have chosen as target area the Sahara desert, and we have acquired both SEVIRI and IASI data (infrared radiances and cloud mask). The time period considered is that of July 2010 (the whole month). ECMWF analyses for the same date and target area have been also acquired, which comprise T_s, T(p), O(p), Q(p) for the canonical hours 0:00, 6:00, 12:00 and 18:00. Moreover, for the purpose of developing a suitable background for emissivity, we have used the Global Infrared Land Surface Emissivity database developed at CIMSS, University of Wisconsin, that is derived by MODIS observations and is available from the year 2003 till 2011.

Keywords. IASI in synergy with other instruments; Retrieval Techniques.

1. Introduction

Nowadays the retrieval of geophysical parameters from satellite observations largely relies on a-priori information, which is derived from climatology and/or models for Numerical Weather Prediction. Thus, the retrieval problem can be efficiently analyzed within the broad context of data assimilation, which is indeed the paradigm of the many seemingly different methods, which have been developed over the past years. The Bayes theorem and its formalism offer a unifying framework for all these techniques, indeed Variational methods, Optimal Estimation, Kalman Filter, Kriging or optimal spatio-temporal interpolation end up with the same formal solution as far as the estimate of geophysical parameters is concerned. This unified picture allowed us to pick up the most general methodologies in order to better take into account for the inclusion of spatio-temporal constraints.

The Kalman filter and optimal estimation with the strategy of accumulating the observation during the day are the most natural tools to consider time-evolution, spatial variability is still to be ex-

ternally included through a suitable definition of the background covariance matrix, which inevitably increases the dimension of the state vector. Thus, in the end the problem is fundamentally one of data-dimension reduction.

To date, this problem is mostly dealt with suitable orthogonal transforms, which can allow us to compress much of the data and state vector information in few coefficients of the expansion.

The present study wants to define a suitable retrieval methodology for the infrared channels of the Meteosat Second Generation (MSG) SEVIRI (Spinning Enhanced Visible and Infrared Imager), identifying a retrieval case of study for surface emissivity and temperature in order to exemplify the strategy of how to consider the spatio-temporal variability of the data. Finally, these retrievals are compared with IASI (Infrared Atmospheric Sounding Interferometer) ones.

IASI has been developed in France by the Centre National d'Etudes Spatiales (CNES) and is flying on board the Metop-A (Meteorological Operational Satellite) platform, the first of three satellites of the European Organization for the Exploitation of Meteorological Satellite (EUMETSAT) European Polar System (EPS). Its main objective is to provide suitable information on temperature and water vapor profiles. The instrument has a spectral coverage extending from 645 to 2760 cm^{-1}, which, with a sampling interval $\Delta\sigma = 0.25\ cm^{-1}$, gives 8461 channels for each single spectrum.

Data samples are taken at intervals of 25 km along and across track, each sample having a minimum diameter of about 12 km. With a swath width on Earth's surface of about 2000 kilometers, global coverage is achieved in 12 hours, during which the instrument records about 650000 spectra. Further details on IASI and its mission objectives can be found in [1].

The retrieval of surface and atmospheric parameters from IASI spectral radiances is carried out with a package that we call ϕ-IASI, whose methodological aspects and validation have been described in many papers [2, 3, 4, 5, 6, 7, 8, 9, 10, 11, 12, 13, 14, 15, 16].

The SEVIRI instrument has instead eight infrared channels: 13.4 (746.30), 12.0 (833.33), 10.8 (925.90), 9.7 (1030.9), 8.7 (1149.40), 7.3 (1369.9), 6.2 (1612.9), 3.9 (2564.10) μm (cm^{-1}), respectively. For the last channel we have not developed a radiative transfer model for different reasons which can add a potential large bias, such as channel 3.9 μm is too much broad, it is contaminated from solar emission in daytime, etc. The time resolution of the data is 15 min, whereas each pixel has a size of $3\times3\ Km^2$. In order to obtain a simplified derivation of the radiance (σ-SEVIRI), two types of reflections are used: specular and Lambertian reflection. The forward model σ-SEVIRI is derived from the σ-IASI monochromatic radiative transfer for fast computation of spectral radiance and its derivatives (Jacobian) with respect to a given set of geophysical parameters.

Section 2 describes the data space and the methods used to apply spatio-temporal constraints for surface emissivity and temperature retrievals.

Application to real SEVIRI observations and results concerning daily maps of emissivity and temperature are shown in section 3.

Conclusions and recommendations in perspective for the METEOSAT Third Generation (MTG) Infrared Sounder are taken in section 4.

2. Methods

The target area extends from 15° of West to 10° of East longitude and from 25° to 45° of North latitude (Fig. 1). This selection has been made for the presence of both vegetation and bare soil and desert sand: for bare soil, emissivity variations are very low in the time; for desert sand, we have a role similar to that of truth data thanks to the unique spectral fingerprint in the atmospheric window due to the quartz, of which these areas are rich.

Figure 1. Target Area

SEVIRI observations (Meteosat 9 high rate SEVIRI level 1.5 image data) have been acquired for the target area for the whole month of July 2010.

Ancillary information about the atmospheric component have been also acquired, used as a first guess for the surface and atmospheric parameters. For this purpose ECMWF analyses have been utilized, that is the state vector composed of T_s, T(p), O(p), Q(p) for the canonical hours 0:00, 6:00, 12:00 and 18:00, with an horizontal spatial resolution of 0.5 x 0.5 degrees. In each ECMWF grid box there are on average ≈ 200 SEVIRI pixels. A linear interpolation of this state vector has been made on the temporal MSG resolution grid (acquisition each 15 minutes, for a total of 96 daily time points).

In order to build up the emissivity background, we have used the emissivity database of the Global Infrared Land Surface Emissivity (e.g. http://cimss.ssec.wisc.edu/iremis/) developed at CIMSS, University of Wisconsin [17]. In doing so, we have not used July 2010, left for checking/validation. This database is derived by MODIS observations and is available from the year 2003 till 2011. The emissivity is made available on monthly basis, at 10 wavelength points (or hinge points) on a 0.05 × 0.05 degree grid. The wavelengths are 3.6, 4.3, 5.0, 5.8, 7.6, 8.3, 9.3, 10.8, 12.1, and 14.3 μm. The emissivity cannot be straightly interpolated to the SEVIRI channels, because of the different spectral response function between MODIS and SEVIRI.

This problem has been handled by developing a suitable software, which first extrapolates the low spectral resolution emissivity spectrum to the IASI wavenumber range, and second, through convolution with the SEVIRI spectral response, to the SEVIRI channels (Fig. 2). In this way we have estimated the emissivity a-priori covariance matrix for each point of the SEVIRI grid on the target area, useful to introduce spatial variability for the Optimal Estimation and Kalman filter methodologies, shown below.

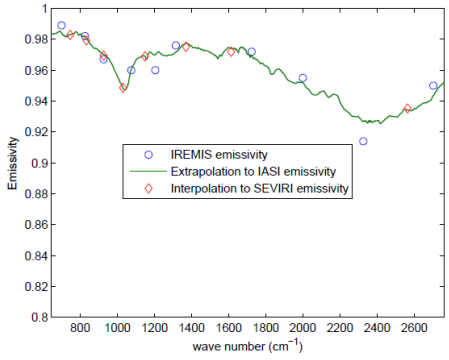

Figure 2. From IREMIS to SEVIRI emissivity, passing through IASI

An example of SEVIRI emissivity retrieval @8.7 μm is depicted in Fig. 3.

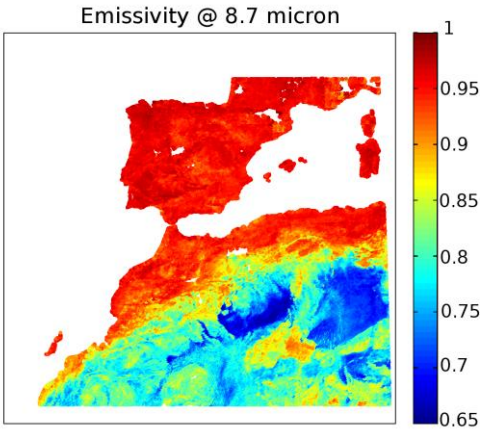

Figure 3. Monthly SEVIRI emissivity retrieval @8.7 μm (July 2010)

2.1. Optimal Estimation

The Optimal Estimation (OE) allows to accumulate the observations during the day, in order to consider the time-evolution and then to introduce time constraints. For its implementation various strategies have been used with the aim to perform the retrieval, such as the use of different time slot widths on which consider the accumulation of observations and the development of static background covariance matrices with fully dependent/independent or correlated state vectors, either for temperature and emissivity. Data assimilation [18] provides a good paradigm for the many methods we are going to review. In particular the methods that consider the a-priori covariance as a static application data, that is Rodgers's Optimal Estimation [19], 1D to 3D variational analysis [20, 21], and the Maximum Likelihood Estimation approach are formally equivalent [18]. Therefore, in reviewing the basic aspects of the retrieval problem with a static a-priori, we approach the issue from the variational perspective, since it has a more straightforward generalization to the fourth time-dimension. In this way our retrieval problem is comparable to a variational analysis in which a suitable estimation of the state vector is obtained by minimizing the form shown in Eq. (1):

$$\min_{\mathbf{v}}\left[\frac{1}{2}\left(\mathbf{R}-F(\mathbf{v})\right)^{T}\mathbf{S}_{\boldsymbol{\varepsilon}}^{-1}\left(\mathbf{R}-F(\mathbf{v})\right)+\frac{1}{2}\left(\mathbf{v}-\mathbf{v}_{\mathbf{a}}\right)^{T}\mathbf{S}_{a}^{-1}\left(\mathbf{v}-\mathbf{v}_{\mathbf{a}}\right)\right] \quad (1)$$

In which:

R : is the radiance vector
F : is the forward model function
v : is the atmospheric state vector, of size N
v_a : is the atmospheric background state vector, of size N
S_{ε} : is the observational covariance matrix, of size M $\times$ M
S_a : is the background covariance matrix, of size N $\times$ N

We will assume that the variability of emissivity is much slower than that of surface temperature: the emissivity is considered constant on the time span, while the surface temperature can vary free with time.

2.2. Kalman Filter

The Kalman filter (KF) is a linear filter developed by Kalman and Bucy [22, 23]. This filter is summarized with the couple of equations represented in (2), which refers to as the observation equation and the state equation respectively.

$$\begin{cases} \mathbf{R}_t = F(\mathbf{v}_t) + \boldsymbol{\varepsilon}_t \\ \mathbf{v}_{t+1} = \mathbf{H}\mathbf{v}_t + \boldsymbol{\eta}_t \end{cases} \qquad (2)$$

In Eq. 2 H is a linear operator, $\boldsymbol{\varepsilon}_t$ and $\boldsymbol{\eta}_t$ are both independent noise terms of the state vector. It is very important to know that the analysis of the formal solution not depends on the data at previous time but only on that at time *t* (Markov property [24]). We have used a simple persistence model for emissivity and surface temperature since the information content of the observations is very high, thus a simplistic state equation can represent the data very well. For the surface temperature retrieval on land we cannot use the model just mentioned, but an autoregressive model of the second order is implemented, where the coefficients are obtained directly from SEVIRI observations. In fact simple persistence model cannot reproduce the daily cyclic behavior expected in condition of clear sky for land surface, while it is a fair model for sea surface, where thermal inertia of water strongly damps the effect of the solar cycle.

The Kalman filter is able to process sequentially the observations, reducing the dimensionality of the retrieval system and has also the capability to deal with unequally spaced times, allowing the jumping over cloudy periods in order to process only clear sky observations, without the need of re-initialize the filter. This is an advantage of this methodology with respect to Optimal Estimation.

2.3. Application to real SEVIRI observation and IASI-SEVIRI spatial co-location

The two retrieval above-mentioned methodologies have been applied to real SEVIRI observations to three target areas, in Spain, in the Sahara desert in the middle of Algerian desert, and in the ocean near the South of the Sardinia Island. For the sake of brevity we focus our attention to the desert region of Ouargla Province, Algeria, which extends from 4° to 8° of East longitude and from 29° to 33° of North latitude, for the purpose to show the comparisons between emissivity and surface temperature for SEVIRI and IASI at SEVIRI space and time resolution.

In order to compare correctly the SEVIRI retrievals with IASI ones, we have co-located spatially SEVIRI pixels with IASI footprints. In detail, IASI emissivity spectrum has been convolved to SEVIRI channels by means of the following equation:

$$\varepsilon^S(\sigma_{ch}) = ISRF(\sigma_{ch}, \sigma) * \varepsilon^I(\sigma) \qquad (3)$$

Where ε^S is the IASI retrieved emissivity to SEVIRI channels, ε^I is the IASI emissivity to IASI channels and ISRF are the Instrument Spectral Response Function of SEVIRI MSG FM2 in correspondence to infrared channels. The Fig. 4 shows the IASI emissivity retrieved on the SEVIRI ISRF. For the emissivity retrieval we have used the 8.7, 10.8 e 12 μm channels. It is evident that at 1149.4 cm^{-1} there is a spatial variability in the emissivity, which follows the distribution of the richer quartz sand across the desert.

In the box of interest we have also 2 Metop orbits, at 9 AM and at 8 PM, for a total of about 10 IASI scan lines. For every day there are more than 400 IASI footprints (200 day-time, 200 night-time).

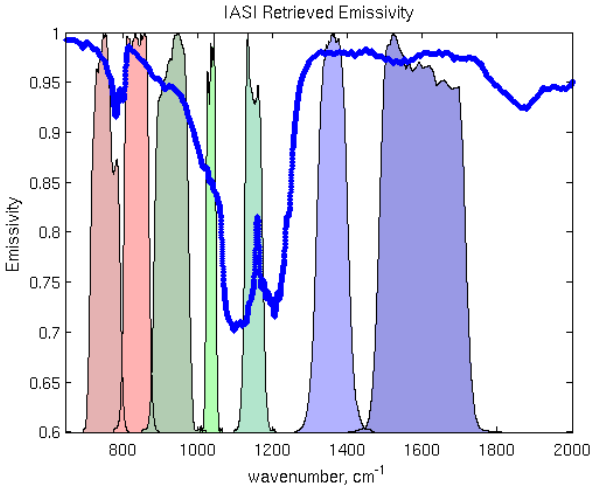

Figure 4. IASI emissivity spectrum on the SEVIRI channels

3. Results

The Kalman filter and the Optimal Estimation methods have been applied to the whole month of SEVIRI observations for the target area shown in Fig. 1, computed at SEVIRI time (15 min) and spatial resolution and then averaged to form daily and monthly maps.

IREMIS database has been used to build up the emissivity background, all but year 2010 used for comparison with the retrieval products. We have been processed only clear sky observations, qualified according to the SEVIRI operational cloud mask [25, 26, 27, 28]. In general both methodologies (KF and OE) agree fairly well with the IREMIS database map, but for the advantages of KF respect with OE (mentioned in Section 2.2), we show only the results obtained with the Kalman Filter applied to SEVIRI observations. Optimal Estimation has instead been used in order to retrieve simultaneously surface temperature, emissivity and atmospheric profiles of temperature, water vapor and ozone from IASI radiances.

In particular we want to compare IASI-SEVIRI retrievals in 2010, July, 10, AM & PM; 2010, July, 4, AM for emissivity and in whole July 2010 for skin temperature. In Fig. 5 the IASI derived SEVIRI channels emissivity is represented for 2010, July, 10, AM & PM.

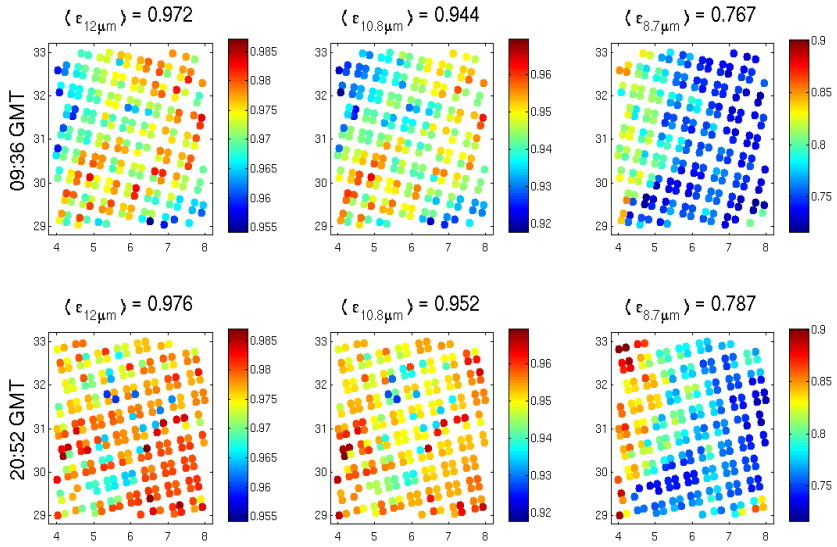

Figure 5. IASI emissivity retrievals on SEVIRI channels (8.7, 10.8 e 12 μm) for 2010, July, 10, AM & PM

In Fig. 6 a) e b) there are the comparisons between IASI (in circles) and SEVIRI both for emissivity and skin temperature in 2010, July, 10, AM and PM respectively.

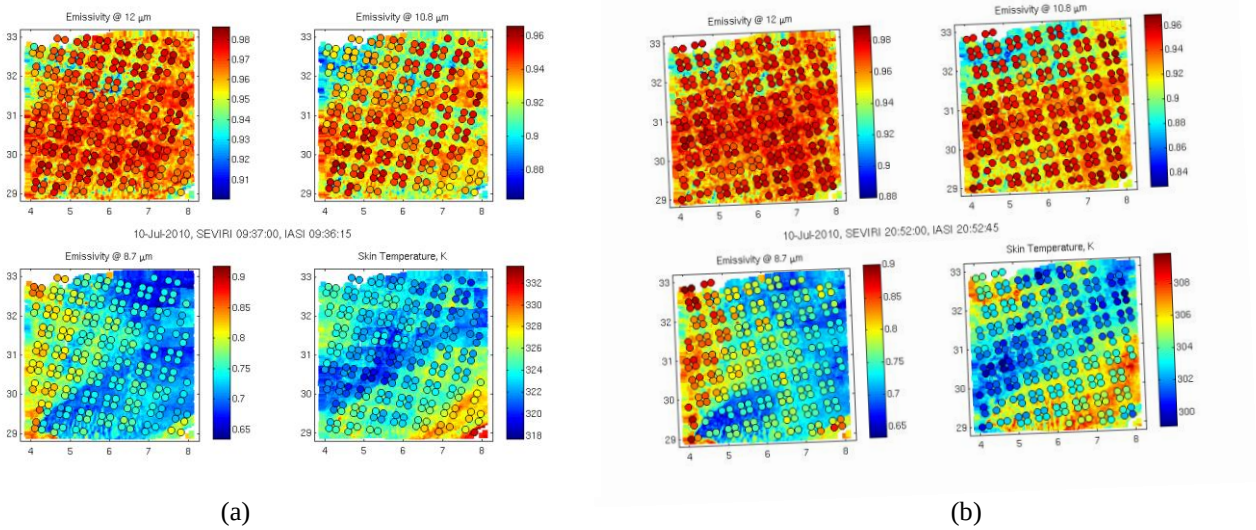

(a) (b)

Figure 6. Comparison between IASI and SEVIRI retrievals in 2010, July, 10, AM (a) & PM (b)

For Fig. 6 (a) 237 IASI spectra have been used, for (b) 246 ones. In Fig. 7 instead we present the histogram of differences for emissivity and skin temperature SEVIRI-IASI for the same data.

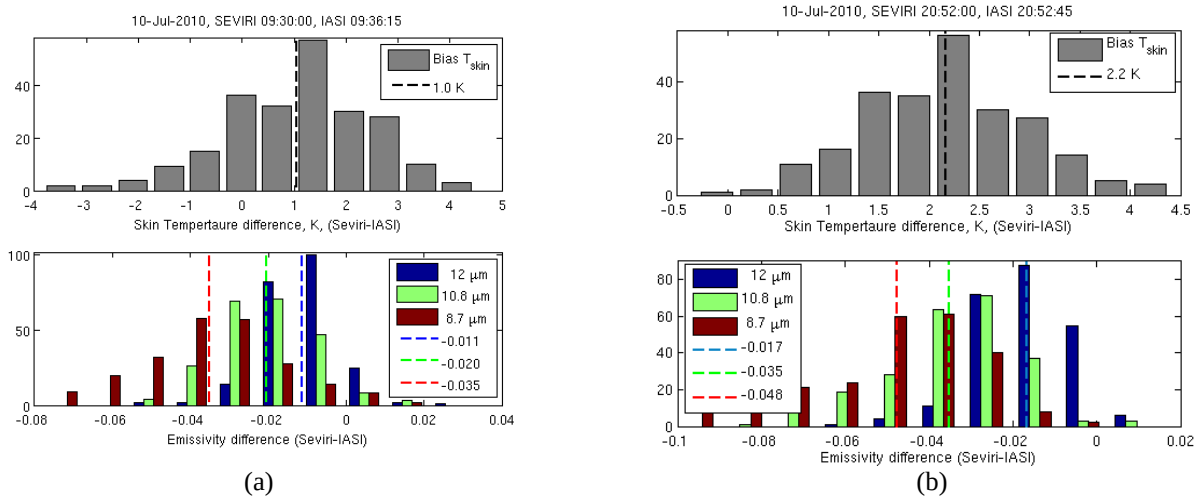

(a) (b)

Figure 7. Histogram of differences between SEVIRI and IASI for skin temperature and emissivity in 2010, July, 10, AM (a) & PM (b)

In order to obtain these comparisons, we have averaged the SEVIRI retrievals (3 x 3 Km) within the IASI pixel (12 x 12 Km) . As depicted in Fig. 7, the mean difference between SEVIRI-IASI skin temperature is about 1 K in daytime and 2.2 K in nighttime, while for emissivity comparison we find a mean difference of 0.02 and 0.035 @ 10.8 μm in day and night time respectively.

These results are very encouraging and the situation improves for the 2010, July, 4, AM with a mean difference of 0.9 K for the skin temperature and of about zero for the emissivity @ 10.8 μm, as shown in Fig. 8 (b). The number of IASI spectra used for these retrievals is 123.

Similar results have been obtained for the other areas of interest.

A very good agreement is also achieved comparing IASI and SEVIRI skin temperature with ECMWF profiles for the whole month of July 2010 (Fig. 9).

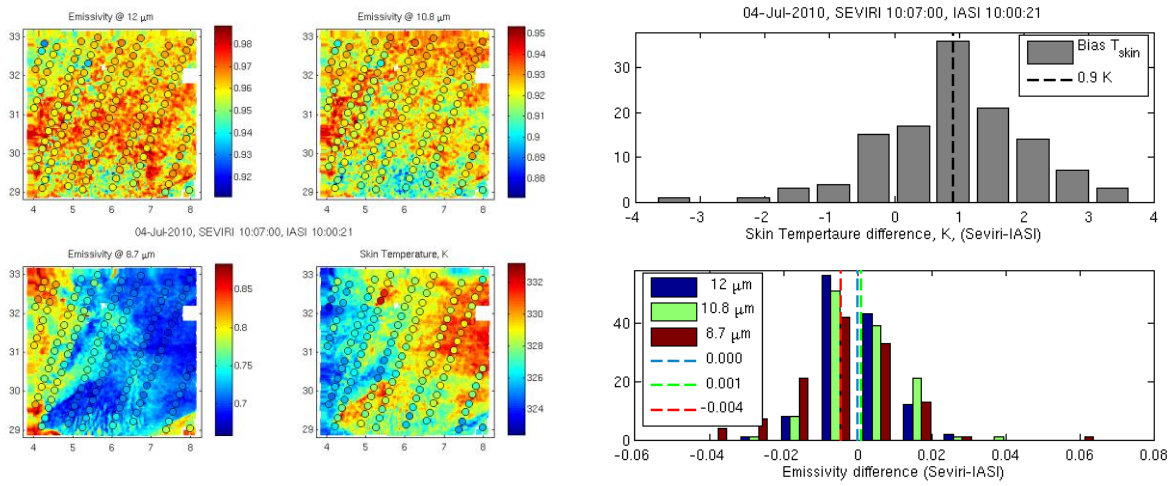

(a) (b)

Figure 8. Comparison between IASI and SEVIRI retrievals in 2010, July, 4, AM (a) and relative histograms of difference for skin temperature and emissivity

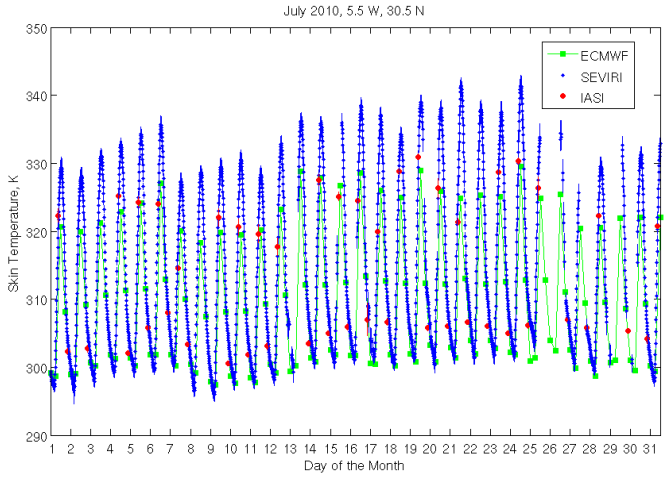

Figure 9. Daily skin temperature for ECMWF (green), SEVIRI (blue) and IASI (red) in the whole month of July 2010

For land surface, OE and KF agree fairly good with ECMWF for nighttime observations, but at midday ECMWF shows a cold bias, which can achieve 10 K and more. This is the case for Spain and Sahara desert. Instead for sea surface OE and KF fairly compare with ECMWF analysis. In this case ECMWF analysis shows a slight warm bias, which by the way is below 0.5 K.

This problem can be justified by the emissivity used for the calculation, extracted from the IREMIS database. It is interesting to note the large sensitivity of the skin temperature on emissivity.

Our emissivity retrieval differs from the IREMIS values for less than 1%, however this cause differences of up to 2-3 K again in the hottest part of the day. In passing, the statistical method seems to give very nice results for Spain. For the Sahara desert the temperature is largely underestimated at midday. Thus ECMWF analyses underestimate of more than 10 K the maximum temperature in the desert areas, while the comparison between IASI and SEVIRI retrievals show a very good agreement.

Furthermore we have demonstrated that there is a variability of emissivity with the diurnal cycle in the desert areas (Fig. 10). This case study has been analyzed by Li et al. [29] which we want to complement and to stress that the observed day/night emissivity variation is due to soil moisture.

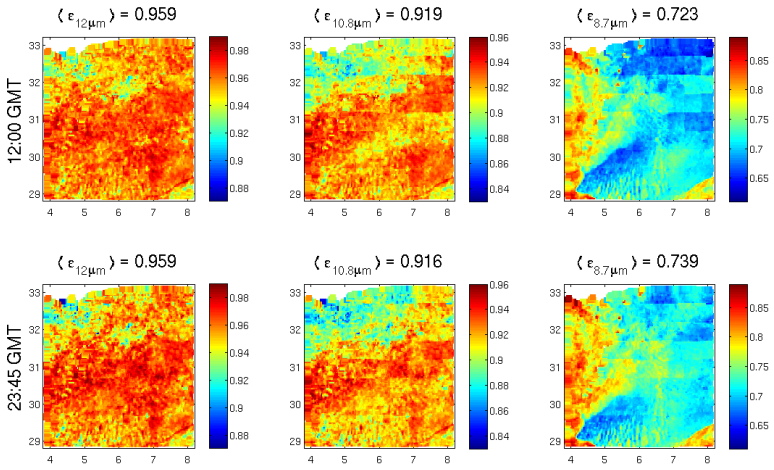

Figure 10. SEVIRI emissivity variability with the diurnal cycle in the Sahara desert

This variability is more evident @ 8.7 μm: the minimum of the emissivity is exactly at midday and it is significant with the well-known diurnal cycle of soil moisture, as shown in Fig. 11.

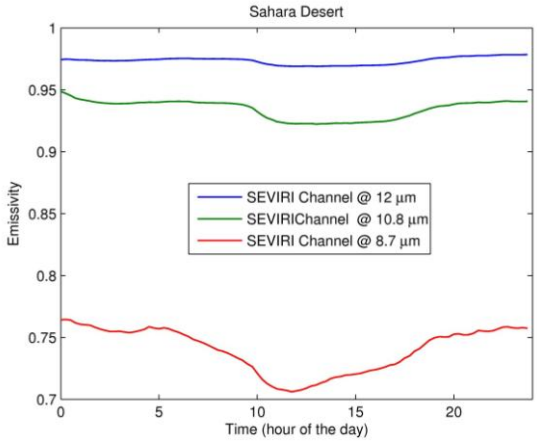

Figure 11. SEVIRI retrieved day/night emissivity versus diurnal cycle in the Sahara desert

This day/night emissivity variability has also been observed in IASI retrieved emissivity spectrum, as depicted in Fig. 12. In red we have drawn the IASI emissivity spectra averaged over 229 footprints recorded during daytime (09:36 GMT), while in blue the IASI emissivity spectra averaged over 205 footprints recorded during nighttime (20:52 GMT) are illustrated.

In detail, Fig. 13 shows the IASI retrieved emissivity variability @ 8.7 μm for the whole month of July 2010. We can conclude saying that the only mechanism responsible of the day/night emissivity variation is the direct water vapor adsorption at the surface.

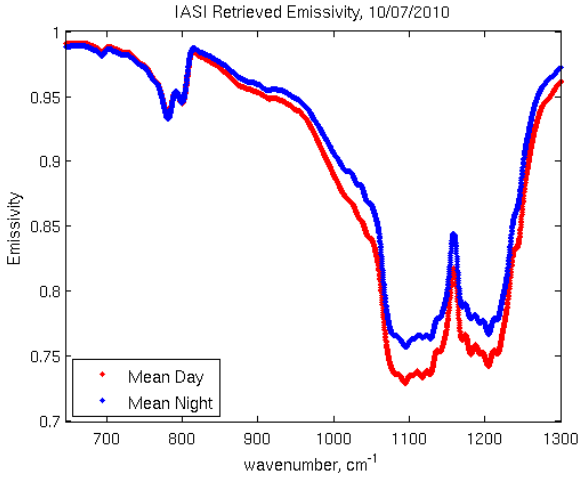

Figure 12. IASI retrieved emissivity spectra for daytime (red) and nighttime (blue) for 10 July 2010

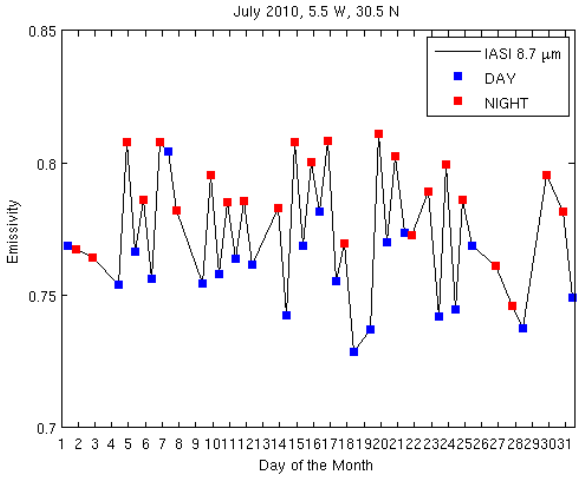

Figure 13. IASI retrieved emissivity spectrum for daytime (blue) and nighttime (red) @ 8.7 µm versus diurnal cycle for the whole July 2010

4. Conclusions

We have reviewed variational and sequential optimal estimation schemes with the objective to apply them to SEVIRI infrared and IASI observations. Specific algorithms have been developed and implemented for the two basic parameters, skin temperature and emissivity.

Concerning the performance of the two applied methodologies, we have that, as far as, the retrieval of skin temperature is concerned, OE and KF are almost equivalent, although a slight bias (of order of 1 K) between the two still persist even on monthly averages. For sea surface we have observed a good agreement between OE and KF retrievals with ECMWF analyses, while for land surface this correspondence is fairly good during nighttime, bur at midday there is a bias of 10 K and more due to ECMWF analyses underestimation.

For emissivity, we have that the comparison with the IREMIS database for the same date and location is fairly good. OE stays closer to IREMIS, whereas KF seems to add independent information of that contained in the IREMIS data base.

On overall the Kalman filter has to be preferred to Optimal Estimation in order to take advantage of time continuity and constraint. In fact with KF it is possible to process time sequences of data points without affecting the dimensionality of the retrieval problem. Even though skin temperature is better represented by a deterministic second-order difference equation, because it is governed by the diurnal cycle, we recommend the use of a persistence model for both sea and land surface. In fact KF can accommodate the state equation or model for the process also when this equation is inherently inadequate to describe the real-world phenomenon. Our confidence about the state equation is inserted through a stochastic variance term, which can trade-off between data and model.

We think that after a training/validation phase, including situations of abrupt changes in surface parameters and/or radiances (e.g. rainfall, cloudiness, weather events) and using truth data, the Kalman approach for the retrieval of Ts− ε from SEVIRI window channels could become operational. We plan to build a full disk SEVIRI emissivity database.

For the problem of deriving a suitable background for emissivity for land surface we definitely recommend to use the UW/IREMIS database.

In perspective for MTG-IRS or geostationary high spectral resolution infrared instruments, one important issue is how to include atmospheric parameters within the retrieved state vector. In this case, a better strategy would be to use a persistence model at each layer and introduce inter-layer correlation through the definition of a proper background as it is done, e.g., with IASI in the context of one-dimensional data assimilation.

Acknowledgements

IASI has been developed and built under the responsibility of the Centre National d'Etudes Spatiales (CNES, France). It is flown onboard the Metop satellites as part of the EUMETSAT Polar System. The IASI L1 data are received through the EUMETCast near real time data distribution service.

References

[1] Hilton, F., Armante, R., August, T., Barnet, C., Bouchard, A., Camy-Peyret, C., Capelle, V., Clarisse, L., Clerbaux, C., Coheur, P.F., Collard, A., Crevoisier, C., Dufour, G., Edwards, D., Faijan, F., Fourri´e, N., Gambacorta, A., Goldberg, M., Guidard, V., Hurtmans, D., Illingworth, S., Jacquinet-Husson, N., Kerzenmacher, T., Klaes, G., Lavanant, L., Masiello, G., Matricardi, M., Mc- Nally, A., Newman, S., Pavelin, E., Payan, S., P´equignot, E., Peyridieu, S., Phulpin, T., Remedios, J., Schl¨ussel, P., Serio, C., Strow, L., Stubenrauch, C., Taylor, J., Tobin, D.,Wolf,W., Zhou, D.: Hyperspectral Earth Observation from IASI: four years of accomplishments. Bullettin of the American Meteorological Society, 93, 347-370, 2012. doi:10.1175/BAMS-D-11-00027.1.

[2] Amato, U., Cuomo, V., De Feis, I., Romano, F., Serio, C., and Kobayashy, H.: Inverting for geophysical parameters from IMG radiances. IEEE Transactions on Geoscience and Remote Sensing, 37, 1620-1632, 1999. doi: 10.1109/36.763277.

[3] Lubrano, A. M., Serio, C., Clough, S.A., and Kobayashy, H.: Simultaneous inversion for temperature and water vapor from IMG radiances. Geophysics Research Letters, 27, 2533-2536, 2000. doi:10.1029/1999GL011059.

[4] Grieco, G., Masiello, G., Matricardi, M., Serio, C., Summa, D., and Cuomo, V.: Demonstration and validation of the ϕ-IASI inversion scheme with NAST-I data, Q. J. R. Meteorol. Soc., 133(S3), 217–232, 2007. doi: 10.1002/qj.162

[5] Amato, U. Antoniadis, A., De Feis, I., Masiello, G., Matricardi, M., and Serio, C.: Technical Note: Functional sliced inverse regression to infer temperature, water vapour and ozone from IASI data, Atmospheric Chemistry and Physics, 9, 5321-5330, 2009. doi:10.5194/acp-9-5321-2009.

[6] Masiello, G., Serio, C., Carissimo, A., Grieco, G., and Matricardi, M.: Application of ϕ -IASI to IASI:

retrieval products evaluation and radiative transfer consistency, Atmospheric Chemistry and Physics, 9, 8771-8783, 2009. doi:10.5194/acp-9-8771-2009.

[7] Grieco, G., Masiello, G., Serio, C.:, Interferometric vs Spectral IASI Radiances: Effective Data-Reduction Approaches for the Satellite Sounding of Atmospheric Thermodynamical Parameters. Remote Sens. 2010, 2(10), 2323-2346, 2010. doi:10.3390/rs2102323.

[8] Masiello, G., Amoroso, M., Di Girolamo, P., Serio, C. Venafra, S., and Deleporte, T.: IASI Retrieval of temperature, water vapor and ozone profiles over land with ϕ-IASI package during the COPS campaign. In Proceedings of the 9th International Symposium on Tropospheric Profiling, ESA, Noordwijk, Netherlands. 2012 (2012c), ISBN/EAN: 978-90-815839-4-7.

[9] Amato, U., Carfora, M.F., Cuomo, V., and Serio, C.: Objective algorithms for the aerosol problem, Appl. Opt. 34, 5442-5452 (1995) *http://www.opticsinfobase.org/ao/abstract.cfm?URI=ao-34-24-5442*

[10] Amato, U.; De Canditiis, D.; Serio, C. (1998). Effect of apodization on the retrieval of geophysical parameters from Fourier-Transform Spectrometers. Appl. Opt., 37, 6537-6543. doi: 10.1364/AO.37.006537

[11] Amato, U., Masiello, G., Serio, C., and Viggiano, M., 2002, The σ -IASI code for the calculation of infrared atmospheric radiance and its derivatives, Environmental Modelling & Software, 17/7, 651 - 667. doi: 10.1016/S1364-8152(02)00027-0

[12] Masiello, G. and C. Serio (2004), Dimensionality-reduction approach to the thermal radiative transfer equation inverse problem, Geophys. Res. Lett., 31, L11105, doi:10.1029/2004GL019845.

[13] Carissimo, A, De Feis, I, Serio, C.(2005). The physical retrieval methodology for IASI: the δ -IASI code. Environ. Modelling & Software, vol. 20/9; p. 1111-1126, doi: 10.1016/j.envsoft.2004.07.003.

[14] Masiello, G.; Matricardi, M.; Serio, C. (2011). The use of IASI data to identify systematic errors in the ECMWF forecasts of temperature in the upper stratosphere. Atmos. Chem. Phys., 11, 1009-1021, doi:10.5194/acp-11-1009-2011.

[15] Masiello, G, Serio, C, Antonelli, P., Inversion for atmospheric thermodynamical parameters of IASI data in the principal components space. Q. J. R. Meteorol. Soc. DOI:10.1002/qj.909 (2011).

[16] Masiello, C., Serio, C., Simultaneous physical retrieval of surface emissivity spectrum and atmospheric parameters from Infrared Atmospheric Sounder Interferometer spectral radiances. Appl. Opt. 52, 2428-2446 (2013) *http://www.opticsinfobase.org/ao/abstract.cfm?URI=ao-52-11-2428* doi: 10.1364/AO.52.002428.

[17] Borbas, E.E. and Ruston, B.C. The RTTOV UWiremis IR land surface emissivity module, NWP SAF, EUMETSAT, 2010.

[18] Wikle, C.K., Berliner, L.M., A Bayesian Tutorial for data assimilation, Physica D, 230 (1-2) pp. 1-26, 2007, doi:10.1016/j.physd.2006.09.017.

[19] Rodgers, C. D., Inverse methods for atmospheric sounding, Theory and Practice World Scientific, Singapore, 2000.

[20] Courtier, P., Variational methods, J. Meteorol. Soc. Jpn 75 (1997) 211218.

[21] Talagrand, O., Assimilation of observations, an introduction, J. Meteorol. Soc. Jpn 75 (1997) 191209.

[22] Kalman, R.E. A new approach to linear filtering and prediction problems. Journal of Basic Engineering 82 (1): 35-45 (1960).

[23] Kalman, R. E., R. S. Bucy. New Results in Linear Filtering and Prediction Theory. Transactions of the ASME - Journal of Basic Engineering 83, 95-107 (1961).

[24] Nychka, D. W. and Anderson, J.L., Data Assimilation, National Center for Atmospheric Research, P.O. Box 3000, Boulder, CO 80307, Draft article for the Handbook on Spatial Statistics (2008).

[25] Serio, C., Lubrano, A., Romano, F., and Shimoda, H.: Cloud Detection Over Sea Surface by use of Autocorrelation Functions of Upwelling Infrared Spectra in the 800-900 cm−1 Window Region, Appl. Opt. 39, 3565-3572 (2000). doi:10.1364/AO.39.003565.

[26] Masiello, G., Matricardi, M., Rizzi, R., and Serio, C.: Homomorphism between Cloudy and Clear Spectral Radiance in the 800-900 cm^{-1} Atmospheric Window Region, Appl. Opt. 41, 965- 973, 2002. doi:10.1364/AO.41.000965.

[27] Masiello, G., Serio, C., and Shimoda, H.: Qualifying IMG Tropical Spectra for Clear Sky. Journal of Quantitative Spectroscopy & Radiative Transfer, 77, 131-148, 2003. doi:10.1016/S0022-4073(02)00083-3.

[28] Masiello, G., Serio, C., and Cuomo, V.: Exploiting Quartz Spectral Signature for the Detection of Cloud-Affected Satellite Infrared Observations over African Desert Areas, Appl. Opt. 43, 2305-2315, 2004. doi:10.1364/AO.43.002305

[29] Li, Z., Li, J., Li, Y., Zhang, Y., Schmit, T.J., Zhou, L., Goldberg, M.D., and Menzel, W.P.: Determining diurnal variations of land surface emissivity from geostationary satellites, J. Geophys. Res., 117, D23302, 2012. doi:10.1029/2012JD018279.